

Ultrasound assisted synthesis of 1-amino-3-ferrocenyl-3-oxoprop-1-enes

Jai N. Vishwakarma*, Shilpika Khanikar, Utpalparna Kalita, Shunan Kaping and Madhushree Ray

Organic Research Lab., Department of Chemical Science, Assam Don Bosco University, Tapesia Campus, Tapesia Gardens, Kamarkuchi, Sonapur-782402, Assam, India

CHRONICLE

Article history:

Received December 22, 2017

Received in revised form

March 20, 2018

Accepted March 25, 2018

Available online

March 25, 2018

Keywords:

Enaminones

Michael addition

Nucleophilic substitution

Crystal structure

ABSTRACT

A clean and efficient, mediated in water and assisted by ultrasound method for the synthesis of a series of *N*-substituted 1-amino-3-ferrocenyl-3-oxoprop-1-enes starting from acetyl ferrocene was developed. Our approach offers shortening of the reaction time under the mild reaction conditions and easy work up procedure.

© 2018 Growing Science Ltd. All rights reserved.

1. Introduction

Studies on the chemistry of ferrocene¹⁻³ have attracted the interest of many scientists and research groups due to its applications in material science,⁴ asymmetric synthesis⁴ and biology.^{5,6} The ferrocene derivatives exhibit also an antiplasmodial,⁷⁻⁹ antitumor,¹⁰ and DNA cleaving¹² activities, have an antiproliferative effects on the MCF7 cell lines,¹¹ activity and have chemotherapeutic action on drug-resistant cancer.^{4,13}

On the other hand, enaminones are important building blocks in the synthesis of many heterocyclic compounds¹⁴ and many therapeutic: antitumor,¹⁵ antimicrobial,¹⁵⁻¹⁷ anticonvulsant,¹⁸ anti-inflammatory,¹⁹ analgesic,¹⁹ ulcerogenic agents.²⁰ Keeping in view the biological importance of enaminones,^{18,21} we have recently reported²² the synthesis of (*Z*)-3-adamantyl-1-aryl-prop-but-2-en-1-ones which were tested for anti-inflammatory and anticancer properties. Also, not much work has been done on the synthesis of enaminones containing the ferrocenyl moiety except for an isolated report on the synthesis of 1-benzylamino-3-ferrocenyl-3-oxoprop-1-ene by Moskalenko *et al.*²⁵ In continuation with our ongoing studies on enaminones²²⁻²⁴ and with the interest in exploring the chemistry of ferrocene due to its unique properties, we decided to develop synthetic strategy for enaminones containing the ferrocene moiety.

* Corresponding author. Fax: +91 361 2841949

E-mail address: jvishwakarma@rediffmail.com (J. N. Vishwakarma)

2018 Growing Science Ltd.

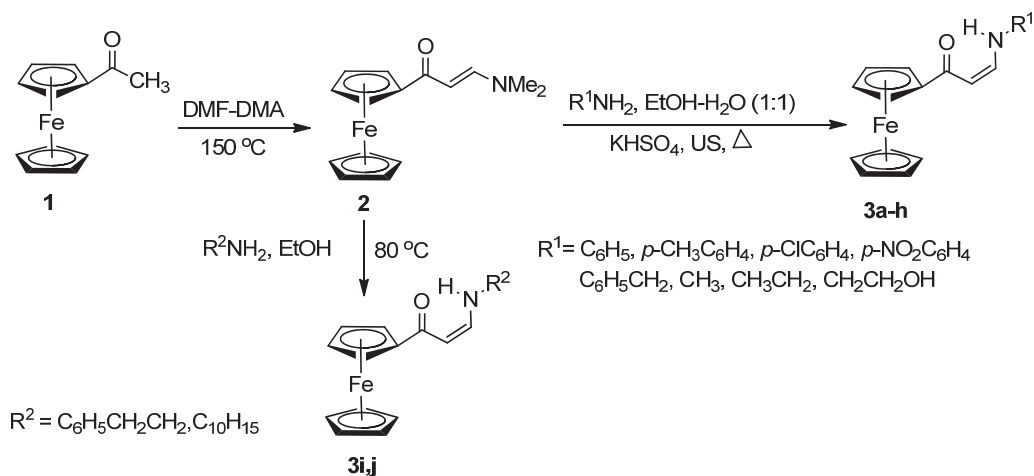
doi: 10.5267/j.ccl.2018.03.001

Ultrasound irradiation offers remarkable effect for the improvement of classical organic reactions.²⁶ Ultrasound reactions work by cavitation process producing localised hot spots with transient high temperature and pressure.²⁷ It offers an alternative source of energy and may reduce the reaction times and enhance the reaction yields under milder conditions.²⁶⁻²⁷

Prompted by these, herein we report the synthesis of 1-amino-3-ferrocenyl-3-oxoprop-1-enes **3(a-j)** under ultrasound irradiation activation in aqueous medium assisted by KHSO_4 .

2. Results and Discussion

In order to synthesize the target enaminones **3(a-j)**, we first formylated 1-acetylferrocene (**1**)²⁵ by reacting with *N,N*-dimethylformamide dimethylacetal (DMF-DMA) to give 1-dimethylamino-3-ferrocenyl-3-oxoprop-1-ene (**2**). The ferrocenyl enaminone **2** was then underwent the reaction with aniline in ethanol: water mixture (1:1) containing KHSO_4 under the ultrasound irradiation at 25 °C to give a precipitated product in 88 % yield. The reaction conditions could easily be extrapolated for the synthesis of **3b–3h** in 75–95 % overall yields (**Scheme 1**). However, the synthesis of **3i** and **3j** could not be achieved under these conditions. They could be synthesised following the conventional method of refluxing in ethanol for 22 hours in 70 and 73 % yields respectively.

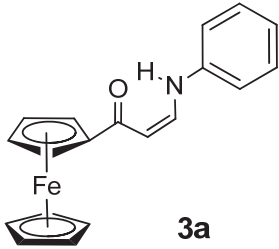
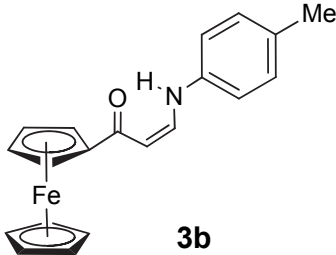
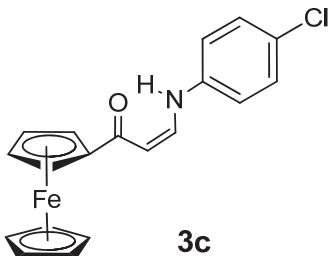
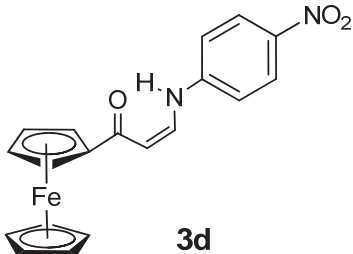


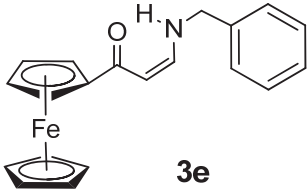
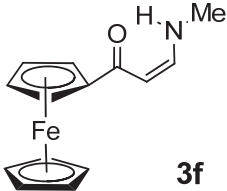
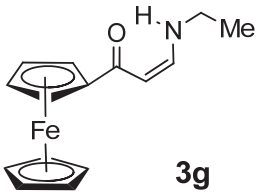
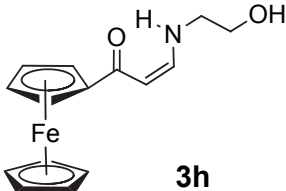
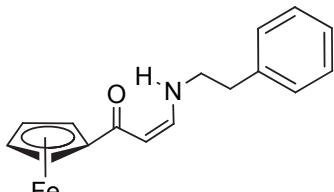
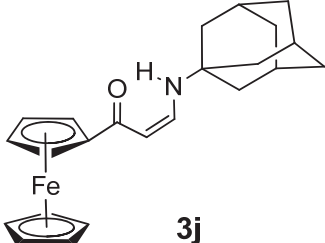
Scheme 1. Synthesis of ferrocenyl enaminone **3(a-j)** from 1-acetylferrocene (**1**)

The structures of the products were established by means of spectroscopic and analytical data. Also, X-ray crystallography for a selected compound **3b** was studied for the final confirmation of the structure. Thus, the IR spectra of **3a–3j** showed characteristic absorption bands due to stretching vibrations of C-H bond of the cyclopentadienyl rings at 2889–3097 cm^{-1} . The carbonyl stretching appeared in the vicinity of 1634 cm^{-1} , while N-H stretching was located in the range of 3263–3442 cm^{-1} . In the proton NMR spectra of **3(a–j)**, the three sets of protons of ferrocenyl group resonated as three distinct singlets around 4.15, 4.38 and 4.71 ppm except in compound **3d** where a set of proton gets merged with the $-\text{CH}_2$ group protons of benzyl and appeared as multiplet in the range 4.37–4.40 ppm. The proton at α -position appeared as doublet ($J \sim 8$ Hz) at about 5.31 ppm due to its coupling with the proton at β -position which itself resonated as multiplet at about 7.26–7.35 ppm for compounds (**3a–3d**) with the aryl group and 6.64–6.96 ppm for compounds (**3e–3i**) with alkyl substituents. In the case of compound **3j**, the β -proton clearly appeared as doublet of doublets ($J \sim 6, 12$ Hz) due to its coupling with the α -proton as well as its additional coupling with N-H proton. While, aromatic protons appeared in their usual range, the NH signal was recognized as broad doublet close to 9.85 ppm for compounds **3e–3i** and as doublet with coupling constant 12 Hz at 11.78 ppm for compounds **3a–3d, 3j**. Further, the structures of the compounds were well supported by mass spectrometry.

In the ^{13}C NMR spectra of these products, the most significant signals were due to carbonyl carbon at 192.5–195.7 ppm. The ferrocenyl carbon atoms resonated at 68.8, 70.1, 71.2, 81.5, 96.1 ppm in compound **3a–3e**, **3h** and at around 68.5–68.7, 69.8–69.9, 70.2–70.9, 71.0–71.1 and 82.3–91.4 ppm in compounds **3f**, **3g**, **3i**, **3j**. In compound **3j** the signals due to adamantyl group carbon atoms appeared as expected at 29.4, 36.2, 43.5 and 52.1 ppm. The synthesised ferrocenyl enaminones are presented in **Table 1**.

Table 1. Synthesis of N-substituted 1-amino-3-ferrocenyl-3-oxoprop-1-enes **3a–3j**

Entry	Compound	Reaction time, min	°C	Yield, %
1	 3a	1	152	88
2	 3b	1	178-180	95
3	 3c	1.5	183-185	80
4	 3d	2	>240	78

5	 <p style="text-align: center;">3e</p>	21	132-135 (184-186) ²⁵	91
6	 <p style="text-align: center;">3f</p>	30	130-132	75
7	 <p style="text-align: center;">3g</p>	9	123-126	70
8	 <p style="text-align: center;">3h</p>	12	120-122	74
9	 <p style="text-align: center;">3i</p>	22*	123-125	78
10	 <p style="text-align: center;">3j</p>	22*	207-208	73

*-hours

Crystal structure of 1-*p*-tolylamino-3-ferrocenyl-3-oxoprop-1-ene (**3b**)

Crystals suitable for X-ray crystallographic study were obtained by the slow crystallisation of **3b** from ethylacetate. The CCDC reference number for the crystallographic data of the structure is 1401880. The crystal belongs to monoclinic, space group P2(1)/c with $a = 19.8419 (5) \text{ \AA}$, $b = 7.5584 (2) \text{ \AA}$, $c = 11.3131 (3) \text{ \AA}$, $\beta = 105.362 (2)^\circ$, $V = 1636.04 (7) \text{ \AA}^3$ and $Z = 4$. The molecular graphic was performed using ORTEP-3 and displacement ellipsoids are drawn at 30 % probability level (**Fig. 1**).

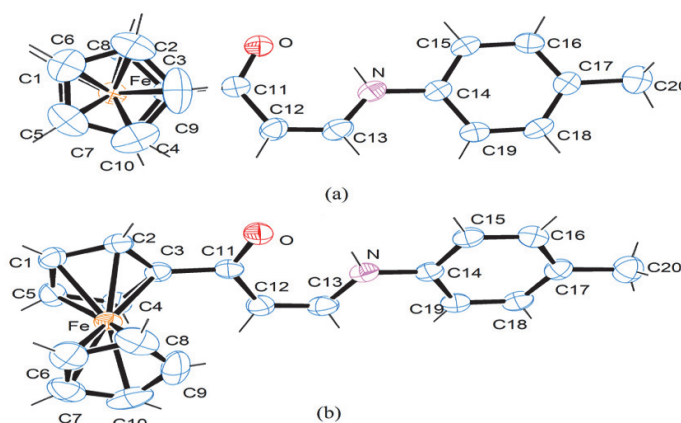


Fig. 1. ORTEP structure of **3b** (a) top view and (b) side view. Ellipsoids are drawn for 30 % probability

Table 2. General and crystal data and summary of intensity data collection and structure refinement for compounds **3b**

Compound No.	3b	Compound No.	3b
Formulae	C ₂₀ H ₂₀ FeNO	F(000)	723.9
Mol. wt.	346.22	Scan type	phi and ω
Crystal system	Monoclinic	Total no. of reflections	24578
Space group	P2 ₁ /c	Observed reflections	2580
<i>a</i> / Å	19.8419 (5)	Independent reflections	4070
<i>b</i> / Å	7.5584 (2)	θ range	2.9–23.7°
<i>c</i> / Å	11.3131 (3)	Ranges (h, k, l)	-26 ≤ h ≤ 26 -10 ≤ k ≤ 10 -15 ≤ l ≤ 14
α/°	90.00	Refinement method	Full-matrix least-squares on <i>F</i> ²
β/°	105.362 (2)	Restraints/Parameters	0/ 256
γ/°	90.00	<i>R</i> [<i>F</i> ² > 2σ(<i>F</i> ²)]	0.040
<i>V</i> / Å ³	1636.04 (7)	Δρ (max;min), e. Å ⁻³	0.32, -0.24
<i>Z</i>	4	Goodness-of-fit = <i>S</i>	1.07
Density/Mgm ⁻³	1.41	<i>R</i> indices (all data)	0.044
Abs. Coeff. /mm ⁻¹	0.925	<i>wR</i> (<i>F</i> ²)	0.110

A summary of the crystal data and experimental detail are given in **Table 2**. Selected bond lengths and bond angles are given in **Table 3** and **Table 4**.

Table 3. Selected bond lengths **3b** (Å)

Bonds	Distance	Bonds	Distance
H5-C5	0.96(3) 1	Fe-C3	2.038(2) 1
H-N	0.88(3) 1	Fe-C1	2.059(4) 1
H12-C12	1.02(3) 1	Fe-C6	2.035(4) 1
C9-C10	1.427(7) 1	Fe-C7	2.030(4) 1
N-C14	1.421(4) 1	C12-C13	1.362(5)
N-C13	1.333(4) 1	C20-H20A	0.960(4) 1
C2-C3	1.429(4) 1	C9-C8	1.391(7) 1
C2-C1	1.415(4) 1	C17-C18	1.390(3)
O-C11	1.248(3) 2	C17-C20	1.512(4) 1
C11-C3	1.486(4) 1	C16-H16	0.929(2) 1
C11-C12	1.424(4)	C14-C19	1.386(3)

Compound **3b** displays hydrogen bonding between N–H··O (**Fig. 2**) with a bond distance of 2.056 Å and thus attains the *Z* configuration. The bond angles of C2–Fe–C3, C14–N–C13, O–C11–C3, C2–

C3–C11 and N–C14–C19 are 40.9, 126.5, 118.8, 124.6 and 123.3 respectively. The molecule as a whole adopts a planar configuration with the torsion angles C2–C3–C11–C12, C13–N–C14–C15, C11–C12–C13–N as 166.1, -170.9 and -1.5 respectively. It can be seen that there is no puckering of the rings, or departure from planarity of any atoms of the cyclopentadienyl rings. The C–C bonds of the cyclopentadienyl ring are almost of the same lengths, approximately 1.42 Å and the C–C–C bond angles almost approximately 108.0° which are not significantly different from the tetrahedral angle 109.5°. The average Fe–C bond was found to be 2.03 Å which is similar to those ferrocene derivatives reported.²⁸ The C–C bond length of the aryl group was found to be approximately 1.38 Å as expected due to the delocalisation of electrons. The bond lengths of O–C11, C11–C12, C12–C13 and C13–N are 1.24, 1.42, 1.36, 1.33 Å respectively.

Table 4. Selected bond angles for **3b** (°)

Bond Angles	Distance	Bond Angles	Distance
C2-Fe-C3	40.9(1)	C14-N-C13	126.5(2)
C2-Fe-C9	123.9(2)	H4-C4-C3	126(2)
H-N-C14	117(2)	H6-C6-C8	124(2)
H-N-C13	116(2)	C14-C19-H19	120.1(2)
O-C11-C12	122.7(2)	H13-C13-N	113(2)
C3-C11-C12	118.5(2)	H13-C13-C12	122(2)
N-C14-C19	123.3(2)	N-C13-C12	125.1(3)
C16-C17-C20	121.6(2)	H12-C12-C13	115(2)
C19-C14-C15	118.5(2)	H5-C5-C4	125(2)
C2-C3-C4	107.4(2)	H20A-C20-H20B	109.5(3)
C2-C1-C5	108.3(3)	C17-C20-H20A	109.4(3)
O-C11-C3	118.8(2)	C2-C3-C11	124.6(2)

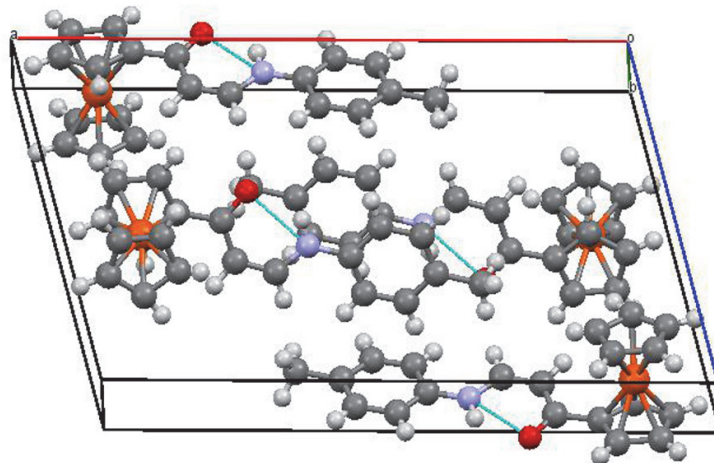


Fig. 2. Packing diagram of compound **3b**. Intramolecular hydrogen bonding shown by the broken lines

3. Conclusions

We have developed a facile synthetic route to enaminones containing the ferrocenyl moiety. The synthetic protocol involving ultrasound irradiation offers several advantages like short reaction time, high yield, mild reaction conditions, easy work-up with high degree of purity. Also, water being used as solvent make this method very convenient and efficient.

Acknowledgements

Authors wish to thank Rev. Fr. Dr. Stephen Mavely, Vice Chancellor, Assam Don Bosco University for providing infrastructure for the execution of this work. Authors also wish to express their gratitude to IIT-Guwahati for providing spectral and analytical data. Our thanks are also due to the Department of Biotechnology (DBT), Government of India for a research grant. UK & SK thank DBT-GOI for research fellowships.

4. Experimental

4.1. Materials and Methods

Melting points were recorded by open capillary method and are uncorrected. The IR spectra were recorded on a fourier transform infrared spectroscopy (FTIR), Perkin Elmer spectrometer in KBr. ^1H NMR (400 MHz), ^{13}C NMR (100 MHz) were measured on a DRX-400 Varian spectrometer and ^1H NMR (600 MHz), ^{13}C NMR (150 MHz) were recorded using a Bruker spectrometer. The chemical shifts (δ ppm) and the coupling constants (Hz) are reported in the standard fashion with reference to TMS as internal reference and CDCl_3 as solvent. The crystallographic data for the structure were deposited to the Cambridge Crystallographic Data Center (CCDC no.1401880). The X-ray diffraction data were collected at 296 K with Mo $K\alpha$ radiation ($\lambda = 0.71073 \text{ \AA}$) using a Bruker Nonius SMART APEX II CCD diffractometer equipped with a graphite monochromator. The structures were solved by direct methods (SHELXS97) and refined by full-matrix least-squares based on F square. All calculations were carried out using WinGX system version 1.80.05. All the non-H atoms were refined in the anisotropic approximation: H-atoms were located at calculated positions. The electron spray mass spectra were recorded on a THERMO Finnigan LCQ Advantage max ion trap mass spectrometer. High resolution mass spectra (HRMS) were recorded on Agilent-Q-TOF 6500 instrument (ESI +ve mode). In spectral data dd, bs, s, d, m, Fc stands for double-doublet, broad singlet, singlet, doublet, multiplet and ferrocene, respectively. Ultrasound irradiation was carried out in an EQUITRON Digital Ultrasonic Cleaner- 2.5 litre, model 8425.025.424 at 170 watt and 50 Hz.

4.2.1 Synthesis of compound 2

Formylation of 1-acetyl ferrocene was carried out following the method as reported by Moskalenko et al.²⁵.

4.2.2 General procedure of synthesis of 1-amino-3-ferrocenyl-3-oxoprop-1-enes (3a-3j)

To a mixture of ferrocenyl enaminone **2** (1 mmol) and primary amine (1 mmol) in 5 cm³ ethanol: water mixture (1:1), KHSO_4 (2 mmol) was added and the resulting mixture was subjected to ultrasound irradiation at 60 °C for 1–30 minutes (**Scheme 1**). After the completion of the reaction (monitored by TLC), the reaction mixture was allowed to cool and the precipitated product (**3a–3h**) was collected by filtration, washed with ethanol: water mixture (1:1) and dried over anhydrous CaCl_2 .

For compounds **3i**, **3j** the reaction did not go to completion under similar conditions and therefore was refluxed in ethanol for 22 hours, whereby the desired products were obtained. On completion of the reaction, ethanol was removed and triturated with hexane to give the crude products. Purification of the products was achieved by column chromatography (silica gel, 5 % EtOAc-Hexane).

4.3 Physical and Spectral Data

1-Anilino-3-ferrocenyl-3-oxoprop-1-ene (3a, $\text{C}_{19}\text{H}_{16}\text{FeNO}$)

Brown solid (291 mg, 88 %); m.p.: 152 °C; ^1H NMR (400 MHz, CDCl_3) δ = 4.19 (s, 5H, C_5H_5); 4.46 (s, 2H, C_5H_2); 4.79 (s, 2H, C_5H_2); 5.59 (d, 1H- αH , $J = 8 \text{ Hz}$); 7.01–7.06 (m, 3H, phenyl); 7.26–7.36 (m, 3H; 2H-phenyl, 1H- βH); 11.78 (d, 1H, NH, $J = 12 \text{ Hz}$); ^{13}C NMR (CDCl_3 , 100 MHz) δ ppm: 68.9, 70.1, 71.7, 81.5 (ferrocene-CH), 95.5 (ferrocene-C), 110.2 ($\alpha\text{-C}$), 115.8, 123.1, 129.8 (aromatic-CH), 140.7 (aromatic-C), 142.1 ($\beta\text{-C}$), 195.4 (carbonyl-C); IR (KBr) ν_{max} = 3423 (NH), 2900 (Fc), 1631 (CO), 1600 (C=C) cm^{-1} ; HRMS (ESI) m/z calcd for $\text{C}_{19}\text{H}_{17}\text{FeNO}$ $[\text{MH}]^+$: 332.0733. Found: 332.0796.

1-*p*-Tolylamino-3-ferrocenyl-3-oxoprop-1-ene (3b, $\text{C}_{20}\text{H}_{18}\text{FeNO}$)

Orange solid (327 mg, 95 %); m.p.: 178–180 °C; ^1H NMR (400 MHz, CDCl_3) δ = 22.30 (s, 3H- CH_3); 4.18 (s, 5H, C_5H_5); 4.44 (s, 2H, C_5H_2); 4.78 (s, 2H, C_5H_2); 5.56 (d, 1H- αH , $J = 8 \text{ Hz}$); 6.96 (s,

2H-phenyl); 7.11 (s, 2H-phenyl); 7.26–7.31 (m, 1H- β H); 11.76 (d, 1H, NH, J = 12 Hz); ^{13}C NMR (CDCl_3 , 100 MHz) δ ppm: 20.9 (methyl-C), 68.8, 70.1, 71.6, 81.9 (ferrocene-CH), 95.0 (ferrocene-C), 110.0 (α -C), 115.9, 130.4, (aromatic-CH), 132.8, 138.3 (aromatic-C), 142.6 (β -C), 195.7 (carbonyl-C); IR (KBr) ν_{max} = 3442 (NH), 2889 (Fc), 1634 (CO), 1550 (C=C) cm^{-1} . HRMS (ESI) m/z calcd for $\text{C}_{20}\text{H}_{19}\text{FeNO}$ $[\text{MH}]^+$: 346.0889. Found: 346.0949.

1-(4-Chlorophenyl)amino-3-ferrocenyl-3-oxoprop-1-ene (3c, $\text{C}_{19}\text{H}_{15}\text{ClFeNO}$)

Brown solid (292 mg, 80 %); mp 183–185 °C; ^1H NMR (400 MHz, CDCl_3) δ = 4.19 (s, 5H, C_5H_5); 4.54 (s, 2H, C_5H_2); 4.80 (s, 2H, C_5H_2); 5.62 (d, 1H- α H, J = 8 Hz); 7.00 (d, 2H-phenyl, J = 8 Hz); 7.34–7.35 (m, 3H, 1H- β H, 2H-phenyl); 11.79 (d, 1H, NH, J = 12 Hz); ^{13}C NMR (CDCl_3 , 100 MHz) δ ppm: 68.9, 70.1, 71.8, 81.3 (ferrocene-CH), 96.1 (ferrocene-C), 112.0 (α -C), 116.9 (aromatic-CH), 127.9 (aromatic-C), 129.8 (aromatic-CH), 139.4 (aromatic-C), 141.7 (β -C), 195.7 (carbonyl-C); IR (KBr) ν_{max} = 3441 (NH), 2900 (Fc), 1635 (CO), 1596 (C=C) cm^{-1} ; HRMS (ESI) m/z calcd for $\text{C}_{19}\text{H}_{16}\text{ClFeNO}$ $[\text{MH}]^+$: 366.0343. Found: 366.0414.

1-(4-Nitrophenyl)amino-3-ferrocenyl-3-oxoprop-1-ene (3d, $\text{C}_{19}\text{H}_{15}\text{FeN}_2\text{O}_3$)

Brown solid (308 mg, 78 %); m.p.: >240 °C; ^1H NMR (400 MHz, CDCl_3) δ = 4.20 (s, 5H, C_5H_5); 4.54 (s, 2H, C_5H_2); 4.81 (s, 2H, C_5H_2); 5.74 (d, 1H- α H, J = 8 Hz); 7.07 (d, 2H-phenyl, J = 8 Hz); 7.33–7.35 (m, 1H- β H); 8.22 (d, 2H-phenyl, J = 8 Hz); 11.99 (d, 1H, NH, J = 12 Hz); ^{13}C NMR (CDCl_3 , 100 MHz) δ ppm: 69.2, 70.3, 72.5, 81.5 (ferrocene-CH), 99.1 (ferrocene-C), 110.8 (α -C), 114.8, 126.3, (aromatic-CH), 133.5, 139.4 (aromatic-C), 142.7 (β -C), 194.1 (carbonyl-C); IR (KBr) ν_{max} = 3437 (NH), 3050 (Fc), 1638 (CO), 1603 (C=C) cm^{-1} ; HRMS (ESI) m/z calcd for $\text{C}_{19}\text{H}_{16}\text{FeN}_2\text{O}_3$ $[\text{MH}]^+$: 377.0584. Found: 377.0541.

1-Benzylamino-3-ferrocenyl-3-oxoprop-1-ene (3e)

Orange solid (313 mg, 91 %); m.p.: 132–135 (Ref [25] 184–186) °C; ^1H NMR (400 MHz, CDCl_3) δ = 4.14 (s, 5H, C_5H_5); 4.37–4.40 (m, 4H, C_5H_2 , 2H- CH_2); 4.71 (s, 2H, C_5H_2); 5.34–5.35 (m, 1H- α H); 6.78–6.81 (m, 1H- β H); 7.28–7.33 (m, 5H-phenyl); 10.11 (bs, 1H, NH); ^{13}C NMR (CDCl_3 , 100 MHz) δ ppm: 52.6 (methylene-C), 68.6, 69.9, 71.2, 82.1 (ferrocene-CH), 92.4 (ferrocene-C), 127.3 (α -C), 127.8, 128.9, 129.0 (aromatic-CH), 138.3 (aromatic-C), 151.8 (β -C), 194.4 (carbonyl-C); IR (KBr) ν_{max} = 3424 (NH), 3000 (Fc), 1631 (CO), 1550 (C=C); HRMS (ESI) m/z calcd for $\text{C}_{20}\text{H}_{19}\text{FeNO}$ $[\text{MH}]^+$: 346.0889. Found: 346.0849.

1-Methylamino-3-ferrocenyl-3-oxoprop-1-ene (3f, $\text{C}_{14}\text{H}_{14}\text{FeNO}$)

Brown flakes (201 mg, 75 %); m.p.: 130–132 °C; ^1H NMR (400 MHz, CDCl_3) δ = .98 (s, 3H- CH_3); 4.11 (s, 5H, C_5H_5); 4.33 (s, 2H, C_5H_2); 4.68 (s, 2H, C_5H_2); 5.25 (d, 1H- α H, J = 8 Hz); 6.64–6.69 (m, 1H- β H); 9.66 (bs, 1H, NH); ^{13}C NMR (CDCl_3 , 100 MHz) δ ppm: 35.3 (methyl-C), 68.6, 69.9, 70.9, 71.1 (ferrocene-CH), 82.3 (ferrocene-C), 91.7 (α -C), 153.2 (β -C), 194.0 (carbonyl-C); HRMS (ESI) m/z calcd for $\text{C}_{14}\text{H}_{15}\text{FeNO}$ $[\text{MH}]^+$: 270.0576. Found: 270.0538.

1-Ethylamino-3-ferrocenyl-3-oxoprop-1-ene (3g, $\text{C}_{15}\text{H}_{16}\text{FeNO}$)

Brown flakes (198 mg, 70 %); m.p.: 123–126 °C; ^1H NMR (400 MHz, CDCl_3) δ = 1.21–1.22 (m, 3H- CH_3); 3.24 (s, 2H- CH_2); 4.14 (s, 5H, C_5H_5); 4.35 (s, 2H, C_5H_2); 4.71 (s, 2H, C_5H_2); 5.26 (d, 1H- α H, J = 8 Hz); 6.72–6.76 (m, 1H- β H); 9.84 (bs, 1H, NH); ^{13}C NMR (CDCl_3 , 100 MHz) δ ppm: 16.8 (methylene-C), 43.7 (methyl-C), 68.5, 69.9, 70.9, 71.1 (ferrocene-CH), 82.3 (ferrocene-C), 91.4 (α -C), 151.6 (β -C), 193.9 (carbonyl-C); IR (KBr) ν_{max} = 3263 (NH), 3097 (Fc), 1635 (CO), 1546 (C=C) cm^{-1} ; HRMS (ESI) m/z calcd for $\text{C}_{15}\text{H}_{17}\text{FeNO}$ $[\text{MH}]^+$: 284.0733. Found: 284.0695.

1-(2-Hydroxyethyl)amino-3-ferrocenyl-3-oxoprop-1-ene (3h, $\text{C}_{15}\text{H}_{17}\text{FeNO}_2$)

Brown flakes (221 mg, 74 %); m.p.: 120–122 °C; ^1H NMR (CDCl_3 , 600 MHz) δ ppm: 3.36 (s, 2H- CH_2 -NH); 3.75 (s, 2H- CH_2 -OH); 4.15 (s, 5H, C_5H_5); 4.38 (s, 2H, C_5H_2); 4.79 (s, 2H, C_5H_2); 5.31

(d, 1H- α H, $J = 6$ Hz); 6.78–6.79 (m, 1H- β H); 9.85 (bs, 1H, NH); ^{13}C NMR (CDCl_3 , 150 MHz) δ ppm: 51.5 (–CH₂NH–), 62.6 (–CH₂OH), 68.7, 70.0, 71.1, 82.0 (ferrocene–CH), 92.3 (ferrocene–C), 96.9 (α -C), 152.6 (β -C), 194.6 (carbonyl–C); IR (KBr) $\nu_{\text{max}} = 3383$ (NH), 2924 (Fc), 1634 (CO), 1553 (C=C) cm^{-1} ; HRMS (ESI) m/z calcd for $\text{C}_{15}\text{H}_{17}\text{FeNO}_2$ $[\text{MH}]^+$: 300.0682. Found: 300.0742.

1-(Phenylethyl)amino-3-ferrocenyl-3-oxoprop-1-ene (3i, $\text{C}_{21}\text{H}_{19}\text{FeNO}$)

Brown solid (280 mg, 78 %); m.p.: 123–125 °C; ^1H NMR (CDCl_3 , 600 MHz) δ ppm: 3.36 (s, 2H–CH₂–NH); 3.75 (s, 2H–CH₂–OH); 4.14 (s, 5H, C₅H₅); 4.36 (s, 2H, C₅H₂); 4.71 (s, 2H, C₅H₂); 5.23 (s, 1H- α H); 6.55–6.58 (m, 1H- β H); 7.19–7.20 (m, 1H-phenyl); 7.21–7.24 (m, 2H-phenyl); 7.29–7.32 (m, 2H-phenyl); 9.91 (bs, 1H, NH); ^{13}C NMR (CDCl_3 , 150 MHz) δ ppm: 38.1 (–CH₂–aromatic), 50.9 (–CH₂NH–), 68.6, 69.9, 70.2, 71.0 (ferrocene–CH), 91.9 (ferrocene–C), 114.0 (α -C), 126.7, 128.8, 129.1 (aromatic–CH), 138.5 (aromatic–C), 151.9 (β -C), 192.5 (carbonyl–C); IR (KBr) $\nu_{\text{max}} = 3437$ (NH), 2900 (Fc), 1623 (CO), 1540 (C=C) cm^{-1} ; HRMS (ESI) m/z calcd for $\text{C}_{21}\text{H}_{20}\text{FeNO}$ $[\text{MH}]^+$: 360.1046. Found: 360.1364.

1-(Adamantan-1-yl)amino-3-ferrocenyl-3-oxoprop-1-ene (3j, $\text{C}_{23}\text{H}_{26}\text{FeNO}$)

Orange solid (283 mg, 73 %); m.p.: 207–208 °C; ^1H NMR (CDCl_3 , 600 MHz) δ ppm: 1.64–1.70 (m, 6H–adamantane); 1.82–1.83 (m, 6H–adamantane); 2.14 (s, 3H–adamantane) 4.15 (s, 5H, C₅H₅); 4.34 (s, 2H, C₅H₂); 4.71 (s, 2H, C₅H₂); 5.28 (d, 1H- α H, $J = 6$ Hz); 6.93–6.96 (dd, 1H- β H, $J = 6$ Hz, 12 Hz); 10.17 (d, 1H, NH, $J = 12$ Hz); ^{13}C NMR (CDCl_3 , 150 MHz) δ ppm: 29.4 (3, CH–adamantane), 36.2 (3, CH₂–adamantane), 43.5 (3, CH₂–adamantane), 52.1 (C–adamantane), 68.5, 69.8, 70.8, 71.0 (ferrocene–CH), 91.2 (ferrocene–C), 111.1 (α -C), 146.6 (β -C), 193.5 (carbonyl–C); IR (KBr) $\nu_{\text{max}} = 3440$ (NH), 2925 (Fc), 1628 (CO), 1556 (C=C) cm^{-1} ; HRMS (ESI) m/z calcd for $\text{C}_{23}\text{H}_{27}\text{FeNO}$ $[\text{MH}]^+$: 390.1515. Found: 390.1583.

References

- 1 Kealy T. J., Pauson P. L. (1951) A new type of organo-iron compound. *Nature*, 168 (4285) 1039-1040.
- 2 Miller S. A., Tebboth J. A., and Tremaine J. F. (1952) Dicyclopentadienyliron. *J. Chem. Soc.*, 74, 632-635.
- 3 Bunting H. E., Green M. L. H., Marder S. R., and Thompson M. E. (1992) The synthesis of ferrocenyl compounds with second-order optical non-linearities. *Polyhedron*, 11 (12) 1489-1499.
- 4 Sarhan A. A. O., and Izumi T. (2003) Design and synthesis of new functional compounds related to ferrocene bearing heterocyclic moieties: A new approach towards electron donor organic materials. *J. Organomet. Chem.*, 675 (1-2) 1-12.
- 5 Jin-Peng Z., Jie D., Ning M., Bo J., Li-Chun X., and Shu-Jiang T. (2013) Microwave-assisted aqueous synthesis of 6-ferrocenyl pyridin-2(1H)-one derivative. *J. Heterocycl. Chem.*, 50 (1) 66-70.
- 6 Wei C-W., Peng Y., Zhang L., Huang Q., Cheng M., Liu Y-N., and Li J. (2011) Synthesis and evaluation of ferrocenoyl pentapeptide (Fc-KLVFF) as an inhibitor of Alzheimer's $\text{A}\beta_{1-42}$ fibril formation *in vitro*. *Bioorg. Med. Chem. Lett.*, 21 (19) 5818-5821.
- 7 Domarle O., Blampain G., Agnani H., Nzadiyabi T., Lebibi J., Brocard J., Maciejewski L., Biot C., Georges A. J., and Millet P. (1998) *In vitro* antimalarial activity of a new organometallic analog, ferrocene-chloroquine. *Antimicrob. Agents Chemother.*, 42 (3) 540-544.
- 8 Chim P., Lim P., Sem R., Nhem S., Maciejewski L., and Fandeur T. (2004) The *in-vitro* antimalarial activity of ferrochloroquine, measured against Cambodian isolates of Plasmodium falciparum. *Trop. Med. Parasitol.*, 98 (4) 419-424.
- 9 Wu X., Tiekink E. R. T., Kostetski L., Kocherginsky N., Tan A. L. C., Khoo S. B., Wilairat P., and Go M-L. (2006) Antiplasmodial activity of ferrocenyl chalcones: Investigations into the role of ferrocene. *Eur. J. Pharm. Sci.*, 27 (2-3) 175-187.
- 10 Neuse E. W. (2005) Macromolecular ferrocene compounds as cancer drug models. *J. Inorg. Organomet. Polym. Mater.*, 15 (1) 3-31.
- 11 Castillo-Ramirez J., Echevarría I., Santiago J., Pérez-Torres M., and Rivera-Claudio M. (2013) Synthesis and characterization of ferrocene acetals and evaluation of their antineoplastic properties by using breast cancer cell lines *in vitro*. *Synthesis*, 45 (13) 1853-1856.

- 12 Fruhauf H-W. (1997) *Chem. Rev.*, 97 (3) 523-596.
- 13 Paitayatat S., Tarnchompoo B., Thebtaranonth Y., and Yuthavong Y. (1997) Correlation of antimalarial activity of artemisinin derivatives with binding affinity with ferroprotoporphyrin IX. *J. Med. Chem.*, 40 (5) 633-638.
- 14 Elassar A-Z. A., and El-Khair A. A. (2003) Recent developments in the chemistry of enamines. *Tetrahedron*, 59 (43) 8463-8480.
- 15 Riyadh S. M. (2011) Enaminones as building blocks for the synthesis of substituted pyrazoles with antitumor and antimicrobial activities. *Molecules*, 16 (2) 1834-1853.
- 16 Michael J. P., De Koning C. B., Hosken G. D., and Stanbury T. V. (2001) Reformatsky reactions with *N*-arylpiperidine-2-thiones: synthesis of tricyclic analogues of quinolone antibacterial agents. *Tetrahedron*, 57 (47) 9635-9648.
- 17 Wang Y. F., Izawa T., Kobayashi S., and Ohno M. (1982) Stereocontrolled synthesis of (+)-negamycin from an acyclic homoallylamine by 1,3-asymmetric induction. *J. Am. Chem. Soc.*, 104 (1) 6465-6466.
- 18 Foster J. E., Nicholson J. M., Butcher R., Stables J. P., Edafiogho I. O., Goodwin A. M., Henson M. C., Smith C. A., and Scott K. R. (1999) Synthesis, characterization and anticonvulsant activity of enamines. Part 6: Synthesis of substituted vinylic benzamides as potential anticonvulsants. *Bioorg. Med. Chem.*, 7 (11) 2415-2425.
- 19 El-Sehemi A. G., Bondock S., and Ammar Y. A. (2014) Transformations of naproxen into pyrazolecarboxamides: search for potent anti-inflammatory, analgesic and ulcerogenic agents. *Med. Chem. Res.*, 23 (2) 827-838.
- 20 Dannhardt G., Bauer A., and Nowe U. (1997) Non-steroidal anti-inflammatory agents, Part 24. Pyrrolidino enamines as models to mimic arachidonic acid. *Arch. Pharm.*, 330 (3) 74-82.
- 21 Eddington N. D., Cox D. S., Roberts R. R., Stables J. P., Powell C. B., and Scott K. R. (2000) Enamines-versatile therapeutic pharmacophores. Further advances. *Curr. Med. Chem.*, 7 (20) 417-436.
- 22 Kalita U., Kaping S., Nongkynrih R., Sunn M., Boiss I., Singha L. I., and Vishwakarma J. N. (2015) Synthesis, structure elucidation, and anti-inflammatory/anti-cancer/anti-bacterial activities of novel (*Z*)-3-adamantyl-1-aryl-prop/but-2-en-1-ones. *Med. Chem. Res.*, 24 (1) 32-50.
- 23 Kalita U., Kaping S., Nongkynrih R., Singha L. I., and Vishwakarma J. N. (2015) Novel tetrahydropyrimidine–adamantane hybrids as anti-inflammatory agents: synthesis, structure and biological evaluation. *Med. Chem. Res.*, 24 (6) 2742-2755.
- 24 Devi A. S., Kaping S., and Vishwakarma J. N. (2015) A facile environment-friendly one-pot two-step regioselective synthetic strategy for 3,7-diarylpyrazolo[1,5-*a*]pyrimidines related to zaleplon and 3,6-diarylpyrazolo[1,5-*a*]pyrimidine-7-amines assisted by KHSO₄ in aqueous media. *Mol. Divers.*, 19 (4) 759-771.
- 25 Moskalenko A. I., Boeva A. V., and Boev V. I. (2011) Reaction of acetylferrocene with dimethylformamide dimethyl acetal and some transformations of the reaction product. *Russ. J. Gen. Chem.*, 81 (3) 521-528.
- 26 Buriol L., Munchen T. S., Frizzo C. P., Marzari M. R. B., Zanatta N, Bonacorso H. G., and Martins M. A. P. (2013) Resourceful synthesis of pyrazolo[1,5-*a*]pyrimidines under ultrasound irradiation. *Ultrason. Sonochem.*, 20 (5) 1139-1143.
- 27 Singh B. S., Lobo H. R., Pinjari D. V., Jarag K. J., Pandit A. B., and Shankarling G. S. (2013) Ultrasound and deep eutectic solvent (DES): A novel blend of techniques for rapid and energy efficient synthesis of oxazoles. *Ultrason. Sonochem.*, 20 (1) 287-293.
- 28 Trivedi R., Deepthi S. B., Giribabu L., Sridhar B., Sujitha P., Kumar C. G., and Ramakrishna K. V. S. (2012) Synthesis, crystal structure, electronic spectroscopy, electrochemistry and biological studies of ferrocene–carbohydrate conjugates. *Eur. J. Inorg. Chem.* 2012 (13) 2267–2277.

